DOI: 10.1002/cphc.201001061

Identifying Protein β-Turns with Vibrational Raman Optical Activity

Thomas Weymuth,[a] Christoph R. Jacob,*[b] and Markus Reiher*[a]

β-turns belong to the most important secondary structure elements in proteins. On the basis of density functional calculations, vibrational Raman optical activity signatures of different types of β-turns are established and compared as well as related to other signatures proposed in the literature earlier. Our findings indicate that there are much more characteristic ROA signals of β-turns than have been hitherto suggested. These suggested signatures are, however, found to be valid for the most important type of β-turns. Moreover, we compare the influence of different amino acid side chains on these signatures and investigate the discrimination of β-turns from other secondary structure elements, namely α- and 3_{10}-helices.

1. Introduction

A detailed understanding of the function of any compound (e.g. a catalyst or a protein) goes hand in hand with an elucidation of its structure, conformation, and dynamics. Therefore, the determination of the three-dimensional structure of a given molecule is one of the central tasks in chemistry and biology. Today, there are several different techniques available which allow one to gain considerable insight into the structure of biochemical substances. Well-established among these are X-ray crystallography and nuclear magnetic resonance (NMR) spectroscopy. Additionally, chiroptical techniques (i.e. optical methods able to differentiate between two enantiomers of a chiral substance) such as circular dichroism (CD) or optical rotatory dispersion (ORD) have been used in a wide range of applications such as the determination of the absolute configuration of known or newly synthesized compounds.[1] Most notably, CD spectra of proteins are used to determine the individual amounts of different secondary structure elements such as α-helices or β-sheet structures (e.g. parallel or antiparallel β-sheets) because the signals arising from these structural features can be well distinguished from each other using techniques such as spectral deconvolution.[2]

A promising technique in the vivid field of chiroptical spectroscopy takes advantage of the vibrational Raman optical activity (ROA), which has been predicted by Barron and Buckingham in 1971[3] (based on results obtained by Atkins and Barron in 1969[4]). They showed theoretically that chiral molecules should feature a small difference in the Raman scattering intensities for left and right circularly polarized light. Since then, this effect has first been observed in 1973 by Barron et al.[5] (an observation independently confirmed by Hug et al. in 1975[6]). ROA spectroscopy has matured during the past decades to a routinely applicable technique.[7] It features the general advantages of Raman vibrational spectroscopy, in particular the ability to study biomolecules in their natural environment (i.e. in aqueous solution). Furthermore, vibrational spectroscopy potentially allows for femtosecond time resolution, which is not directly accessible using NMR spectroscopy (a technique featuring typical time scales between 1 s and 1 ps[8]). Since ROA is sensitive to the chirality of a molecule, it adds to these advantages an extra susceptibility to the three-dimensional structure of a molecule. In fact, in ROA only specific information contained in the vibrational spectra is filtered out; thus, the resulting spectra have well-resolved bands in contrast to conventional Raman or infrared (IR) spectra of proteins, which usually suffer from congested line shapes. Very intense ROA signals are often associated with normal modes concerning the most rigid and chiral part of a molecular structure.[7] For proteins, these are usually located within the polypeptide backbone. Thus, it should in principle be possible to obtain information about the conformation of this polypeptide backbone based on characteristic ROA signals.[7] Indeed, efforts have been undertaken to determine the individual amounts of different secondary structure elements in a given protein from its ROA spectrum by means of pattern recognition methods.[9,10]

The identification of signals characteristic for a certain secondary structure element is usually based on the comparison of ROA spectra of proteins and/or model peptides of which the three-dimensional structure was previously elucidated using X-ray crystallography or NMR spectroscopy. Then the secondary structure elements occurring in a certain protein are assumed to be known and by comparison with spectra of proteins featuring similar as well as different secondary structure elements

[a] T. Weymuth, Prof. M. Reiher
ETH Zurich, Laboratorium für Physikalische Chemie
Wolfgang-Pauli-Str. 10, 8093 Zurich (Switzerland)
Fax: (+41) 44 633 15 94
E-mail: markus.reiher@phys.chem.ethz.ch

[b] Dr. Ch. R. Jacob
Karlsruhe Institute of Technology (KIT)
Center for Functional Nanostructures
Wolfgang-Gaede-Str. 1a, 76131 Karlsruhe (Germany)
Fax: (+49) 721 608 48496
E-mail: christoph.jacob@kit.edu

Supporting information for this article is available on the WWW under http://dx.doi.org/10.1002/cphc.201001061.

it is possible to identify band patterns characteristic for a certain secondary structure element. Such investigations have been undertaken since the early 1990s (for a review see, e.g., ref. [7]). However, in such experimental studies one is always restricted in the choice of the compound under investigation. Small oligopeptides are usually very flexible in solution, which leads to a vibrational spectrum averaged over many different conformations, while bigger molecules such as proteins incorporate usually several secondary structure elements, which in turn makes the assignment of a given band to a single secondary structure element difficult. Moreover, since in experimental studies the normal modes are not directly accessible, it is often very challenging, if not impossible, to unequivocally assign a given signal to a distinct vibration. Furthermore, on the basis of experimental investigations it is usually difficult to separate the many different effects influencing the spectra (e.g. the molecular structure, the protein and/or solvent effects, conformational averaging, etc.).

On the other hand, it is possible to calculate ROA spectra of model systems[11–14] that incorporate exactly the desired secondary structure element(s). Such calculations can nowadays be performed on fairly large systems[13,14] and even for small proteins.[15] In such calculations, one has direct access not only to the vibrational wavenumbers and intensities, but also to the corresponding normal modes, that is, the precise motion of the nuclei in each vibration is known. These normal modes can then be further analyzed, for example with the help of localized modes,[16] to obtain additional insights, for example on the dependence of certain vibrations on the molecular conformation. Herein, we choose such a theoretical approach to investigate the ROA spectra of β-turns.

The first study on ROA signatures of β-turns was carried out in 1994 by Wen et al. who investigated the ROA spectra of proteins containing large amounts of antiparallel β-sheets such as α-chymotrypsin (note that the individual β-strands are usually connected by β-turns).[17] They proposed that a negative signal in the range of approximately 1340–1380 cm^{-1} as well as a negative signal at ~1224 cm^{-1} are signatures of β-turns.[17] On the basis of further experimental investigations, the former signal is quite firmly established now.[7,9,18] Furthermore, in 2000 Barron et al. proposed another β-turn signature, namely a positive band in the range of ~1260–1295 cm^{-1}.[7] However, the negative signal at ~1220 cm^{-1} was reassigned to a distinct sort of β-strand or sheet.[7] This was based on the claim that in the ROA spectrum of the capsid of the virus MS2 (an icosahedral bacteriophage), which contains mainly up-and-down β-sheets, such a band would not appear. However, this ROA spectrum was published by the same research group in 2003.[19] A strong negative peak at 1247 cm^{-1} with a shoulder at 1220 cm^{-1} is clearly visible. As a similar negative band at ~1220 cm^{-1} was found in all experimental spectra of proteins containing β-turns,[7,9,15,17–19] there appears to be no reason for this reassignment. However, based on these spectra only it is not possible to determine whether the band at about 1220 cm^{-1} originates from β-sheets or β-turns, as both secondary structure elements occur in these proteins.

A recent theoretical study on the β-domain of rat metallothionein[15] yielded additional insight as this protein contains turns (mostly β-turns) as the only secondary structure element. Thus, any of the ROA signals had to be related either to these turns or to the residual disordered structure. In fact, in the theoretical ROA spectrum of the β-domain of rat metallothionein[15] as well as in the experimental spectrum of rabbit metallothionein[20] a strong negative peak dominating the spectra is visible at 1183 cm^{-1} (together with a smaller peak approximately at 1220 cm^{-1}) and ~1200 cm^{-1}, respectively. Furthermore, both spectra show a strong positive peak at ~1300 cm^{-1}, which could originate in similar normal modes responsible for the positive peak in the range of ~1260–1295 cm^{-1} mentioned above. Finally, a weakly negative peak at 1358 cm^{-1} is visible in the theoretical spectrum of the β-domain of rat metallothionein, but not in the experimental spectrum of rabbit metallothionein where one finds a negative peak only above 1400 cm^{-1}.

In summary, there are three ROA bands which could be assumed to be indicative of β-turns (see Table 1). First, a negative band in the range of ~1200 cm^{-1} and 1220 cm^{-1} (in the following, this signal is referred to as "signature 1" for the sake of brevity), second, a positive signal in the spectral region of ~1260–1300 cm^{-1} (hereafter shortly called "signature 2"), and finally a negative band between ~1340–1380 cm^{-1} (which is denoted as "signature 3"). Herein, we evaluate the validity of these signals on the basis of density functional theory (DFT) calculations on model structures of β-turns. Moreover, we investigate the ROA spectra of these model compounds in order to identify additional signatures for β-turns.

Table 1. Summary of ROA signals which have been proposed to be characteristic for β-turns in the literature.

Signature	Wavenumber Range [cm^{-1}]	ROA Intensity
1	~1200–1220	negative
2	~1260–1300	positive
3	~1340–1380	negative

This work is organized as follows. In Section 2, the model structure setup is rationalized. To this end, the taxonomy of β-turns is briefly reviewed and the previously published calculated ROA spectrum of the β-domain of rat metallothionein is revisited. Next, in Section 3 we explain the methodology used herein to identify β-turn signatures. Then, the calculated spectra are presented and carefully analyzed in Section 4. Finally conclusions together with an outlook are given in Section 5.

2. Model Structure Setup

2.1. Taxonomy of β-Turns

A tight turn is defined as a protein site where the polypeptide chain folds back on itself and the number of amino acid residues directly participating in forming the turn does not exceed six. Additionally, the distance between the C_i^α and the C_{i+3}^α

atoms (here and in the following, the index *i* counts the amino acid residues) has to be smaller than 7 Å.[21] Such turns play an important role as a protein could not reach a compact, globular form without them. Consequently, tight turns have long been recognized as one of the three most important secondary structure elements, the other two being the well-known α-helix and β-sheet structures.

Tight turns are usually classified by the number of residues directly involved in forming the turn. The most important class of tight turns, the β-turns, is constituted of four residues. A schematic representation of a β-turn is shown in Figure 1.

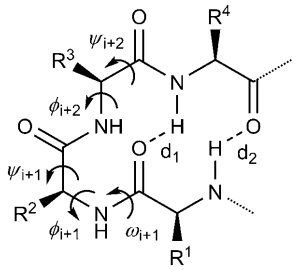

Figure 1. General structure of a β-turn. R^i denotes the amino acid side chains. Important torsional angles are indicated by arrows together with their common designations. Neither of the two intramolecular hydrogen bonds indicated by the dashed lines and labelled d_1 and d_2, respectively, is necessarily expressed in a real turn. The dotted lines indicate the continuation of the polypeptide backbone.

These β-turns can be further classified according to their backbone dihedral angles ϕ_{i+1}, ψ_{i+1}, ϕ_{i+2}, and ψ_{i+2} (see Figure 1). Nowadays, the classification scheme of Hutchinson and Thornton[22] is most widely used for this purpose. Within this scheme, one distinguishes nine different types of β-turns, the idealized backbone dihedral angles of which are given in Table 2 together with their relative occurence. The assignment of any turn to a class is based on its backbone dihedral angles ϕ_{i+1}, ψ_{i+1}, ϕ_{i+2}, and ψ_{i+2} where the angles are allowed to deviate by 30° (one angle is allowed to deviate up to 45°).

As can be seen in Table 2, type I is the most important one. Type IV is a miscellaneous category which contains all turns not fitting into any other class, that is, turns in which at least two torsional angles deviate more than 30° from their corresponding idealized angles and turns in which one backbone dihedral angle deviates more than 45° from its idealized standard value. Therefore, type IV does not correspond to a distinct type of β-turn. It is worth noting that the backbone dihedral angles of types I and I′ as well as types II and II′ β-turns, respectively, feature the same absolute values but opposite signs. Thus, idealized β-turns of types I and I′ or types II and II′ are exact mirror images of each other, provided there is no other source of chirality. In addition to type I, II, I′, and II′, type VIII can also in general be realized for any amino acid sequence. However, in turn types VIa1, VIa2, and VIb, the third residue has to be a proline. Additionally, the second peptide unit features a *cis*- rather than the usual *trans*-geometry. If these two additional criteria are not fulfilled, the distance between the C_i^α and the C_{i+3}^α atoms is bigger than 7 Å.[21]

Table 2. Idealized backbone dihedral angles and occurrence frequencies [%] of β-turns according to the classification Scheme by Hutchinson and Thornton. The occurrence frequencies are based on the original data set of Hutchinson and Thornton.[22]

Turn Type	Relative Occurrence	ϕ_{i+1}	ψ_{i+1}	ϕ_{i+2}	ψ_{i+2}
I	31.75	−60	−30	−90	0
II	10.39	−60	120	80	0
VIII	8.34	−60	−30	−120	120
I′	3.26	60	30	90	0
II′	2.31	60	−120	−80	0
VIa1	0.38	−60	120	−90	0
VIa2	0.13	−120	120	−60	0
VIb	0.90	−135	135	−75	160
IV	42.73				

Even though improved classification schemes have been developed recently,[23] we will adopt the well-known classification scheme by Hutchinson and Thornton as presented in Table 2. Note that this scheme agrees with the one proposed in ref. [23] for all turn types considered herein. Furthermore, we will only concern ourselves with turns belonging to types I, I′, II, II′, or VIII as type IV is a miscellaneous category and types VIa1, VIa2, and VIb occur only seldom and have to fulfill special requirements.

2.2. Turn Signatures in the β-Domain of Rat Metallothionein

One can raise the question whether small model systems include all necessary features of β-turns embedded in larger systems such as proteins. In particular, it is not clear a priori whether the proposed β-turn signatures discussed in the Introduction stem from a collective motion of many turns in the protein or are composed of normal modes involving rather localized vibrations of single turns. To this end, we revisit the calculated ROA spectrum of the β-domain of rat metallothionein,[15] which can be analyzed by inspection of the normal modes in the wavenumber range between 1150 and 1400 cm^{-1}. As has already been stated, this protein contains β-turns as the only secondary structure element. To be more precise, we find two type I β-turns (sequences Asp2–Pro3–Asn4–Cys5 and Cys26–Thr27–Ser28–Cys29, respectively), as well as a type I′ β-turn in the sequence Cys15–Ala16–Gly17–Ser18. In addition, there is a type IV β-turn consisting of residues Cys21–Lys22–Gln23–Cys24.

We find that in almost all cases the normal modes in the region of interest are well localized, that is, only a relatively small and distinct part of the protein is involved in significant vibrations; mostly, not more than about 5–25 atoms are in motion (compared to the total number of 411 atoms). Therefore, we can conclude that the ROA signals characteristic for β-turns originate from vibrations of rather localized parts of a protein; the collective motion of all protein atoms plays only a negligible role. Thus, small model structures do not appear to be too small to explore β-turn signatures. Furthermore, as model systems can be chosen to represent one single β-turn only, we can expect to get pure β-turn signatures from them. Enlarging such models would only increase the amount of

other secondary structure elements or disordered structure, thereby possibly covering or even changing true turn signatures.

Furthermore there are indeed normal modes localized on the β-turns featuring wavenumbers which agree with those of the proposed signatures. For example, normal modes at 1203 cm^{-1}, 1300 cm^{-1}, and 1340 cm^{-1}, respectively, are associated with the first type I β-turn (Asp2–Pro3–Asn4–Cys5), while normal modes with the wavenumbers 1202 cm^{-1}, 1306 cm^{-1}, and 1363 cm^{-1}, respectively, are localized on the second β-turn of type I (Cys26–Thr27–Ser28–Cys29). Finally, normal modes at 1221 cm^{-1}, 1300 cm-1, and 1384 cm^{-1}, respectively, represent vibrations of the type I′ β-turn (Cys15–Ala16–Gly17–Ser18).

Additionally, we find that by far most of the normal modes in the wavenumber range between 1150 and 1400 cm^{-1} of the β-domain of rat metallothionein consist of a combination of CH_2 deformation (stemming from cysteine side chains for example), C^{α}–H bending and NH in-plane bending vibrations. While the latter two are expected in this wavenumber region, it is interesting to note that the CH_2 deformation appears to play an important role here. Already in 1994, Barron and coworkers proposed,[17] based on a normal mode analysis of the crystal structure of melanostatin by Naik and Krimm,[24] that the ROA signatures of β-turns they proposed at that time[17] originate mainly from CH_2 deformations coupled with NH in-plane deformations. To shed further light on this issue, we calculated ROA spectra of β-turns featuring different amino acid side chains.

2.3. Selection of Model Compounds

In order to identify specific ROA signatures of β-turns, we construct fifteen different model systems of true β-turns where we use an oligopeptide consisting of four amino acid residues (either (*S*)-alanine, glycine or (*S*)-cysteine) fitting into types I, I′, II, II′, or VIII. These structures are fully optimized, starting from the idealized angles (see Table 3 for the resulting backbone angles). In the following, we denote each of these model systems by the amino acid it is built from together with the turn type it forms (for example, the model structure Ala-I forms a type I β-turn and is constituted of four (*S*)-alanine residues). Structures of the five (all-*S*)-alanine β-turn models are shown in Figure 2a. The corresponding β-turn models constituted from other amino acid residues have similar peptide backbones. As examples, the different type I β-turn models are shown in Figure 2b.

Table 3. Backbone dihedral angles ϕ_{i+1}, ψ_{i+1}, ϕ_{i+2} and ψ_{i+2} and CO_i-NH_{i+3} distance d_1 as well as NH_i–CO_{i+3} distance d_2 (see Figure 1 for the designation of these distances) of all β-turn models investigated in this work. The values of all angles are given in degrees.

Structure	ϕ_{i+1}	ψ_{i+1}	ϕ_{i+2}	ψ_{i+2}	d_1 [Å]	d_2 [Å]
Gly-I	−69.74	−17.07	−107.02	21.28	1.95	2.21
Gly-II	−66.62	114.13	89.85	−1.62	1.96	2.26
Gly-VIII	−71.02	−24.08	−129.78	144.08	5.11	5.41
Gly-I′	69.74	17.06	107.04	−21.27	1.96	2.21
Gly-II′	66.63	−114.14	−89.85	1.63	1.96	2.26
Ala-I	−67.18	−19.88	−112.60	14.01	2.00	2.37
Ala-II	−64.51	113.39	64.97	18.60	2.02	2.24
Ala-VIII	−84.96	−18.28	−128.73	125.71	5.36	4.83
Ala-I′	57.15	36.95	77.84	−0.22	1.94	2.41
Ala-II′	66.65	−107.37	−100.16	0.82	2.03	2.17
Cys-I	−65.50	−23.13	−110.26	17.10	1.94	2.44
Cys-II	−56.69	129.36	92.95	−14.86	1.93	2.46
Cys-VIII	−88.59	−10.25	−135.41	127.87	5.60	4.21
Cys-I′	40.90	52.54	86.27	−3.80	1.85	2.21
Cys-II′	60.02	−118.06	−97.30	11.43	2.03	2.17

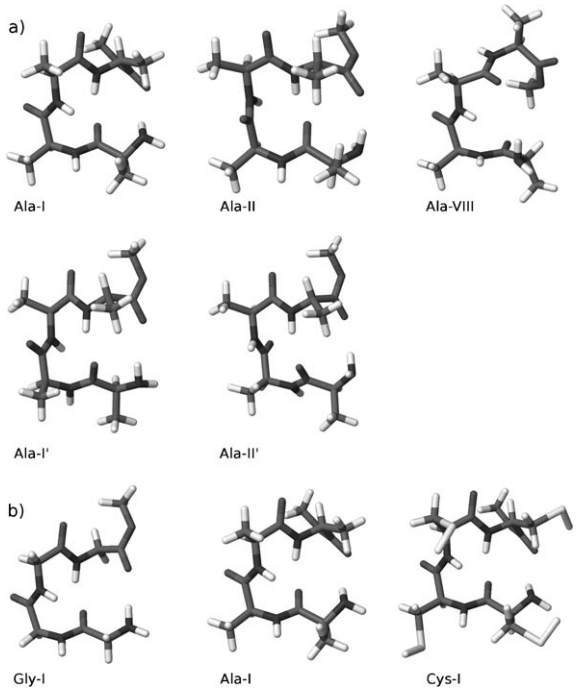

Figure 2. a) Structures of the five (all-*S*)-alanine β-turn models investigated herein; b) Structures of the three type I β-turn models featuring glycine, (*S*)-alanine, and (*S*)-cysteine amino acid residues.

All model systems investigated in this work represent non-solvated β-turns. While such a setup is of course not representative of the native solvated state of these polypeptides it can nevertheless be used to study the generic signals of such β-turns and will allow us to separate the effect of solvation in later studies. For the computational methodology we may refer the reader to a detailed description provided in the Computational Details.

3. Identifying Signatures in Calculated ROA Spectra

The goal of this work is to check the validity of the β-turn signatures suggested so far (summarized in Table 1) as well as to possibly identify additional signatures. Concerning the first point, we check each calculated spectrum individually for the existence of the suggested signatures. A direct approach in order to confirm (or disprove) these β-turn signatures proposed in the literature would be to check whether a suitable band occurs in the given intervals. However, smaller errors

(e.g. wavenumber shifts of individual normal modes) stemming from the simplifications made in order to facilitate the computations (e.g. the neglect of solvent effects) can have rather dramatic influences on the spectra. For example, close-lying negative and positive normal modes can cancel each other, such that no visible band results although a couplet should appear. Herrmann et al. addressed this problem and proposed that the analysis of an ROA spectrum in terms of *total* intensities of given intervals is much more advantageous,[25] as in this case these errors do not matter. Usually these errors are partially eliminated by convoluting the original stick spectrum with a line-broadening function. Here, we use such an approach and compare total intensities integrated over a range of wavenumbers in order to test for the occurence of the proposed signatures. In a next step, we check whether the proposed signatures occur consistently, that is, for different types of β-turns and amino acid residues. It needs also to be stated here that the errors resulting from simplifications (e.g. neglect of solvent effects or of conformational averaging) can be expected to have a similar influence in all spectra. Thus, when comparing the diffferent calculated spectra to each other, characteristic peaks should still appear at similar positions.

In order to identify additional signatures, we can also use the methodology proposed by Herrmann et al.[25] to compare individual spectra to each other in order to find similarities, namely regions where the intensity has the same sign in all spectra. We can then identify these regions as being characteristic for the whole set of model structures which have been studied. To this end, we divide the spectra into intervals of 10 cm^{-1} using a step size of 1 cm^{-1} (e.g. one interval ranging from 1000 to 1010 cm^{-1} while the second interval goes from 1001 to 1011 cm^{-1}) and calculate the total intensity of these intervals by numerically integrating the Lorentz-broadened line function. Doing so, we can identify regions which feature the same sign of the total intensity in all spectra. We chose to calculate the total intensities of these intervals by integrating the Lorentz-broadened line functions instead of simply summing up the intensities of the individual normal modes. In this way the resulting total intensities depend much less on the actual interval width and on the step size.

Once we find regions with the same sign of the total intensity, we check these regions in order to decide whether these could actually represent useful signatures. If this is not the case (for instance, because the intensity is weak, such that the corresponding band could easily be covered, we do not consider it any further.

When spectral features characteristic for (certain kinds of) β-turns have been established, a last question to be answered is whether one can use these as signatures to distinguish β-turns from other secondary structure elements, e.g., α-helices. For this one obviously needs spectral data of such secondary structure elements which can be obtained using experimental as well as theoretical methods. Such data is available in the literature (see, e.g., refs. [7, 14, 26]).

4. Results and Discussion

4.1. Glycine Models

As a starting point, we consider the simplest possible model structure of a β-turn, that is, four glycine residues connected to each other. The ROA spectra of these five glycine β-turn models are shown in Figure 3.

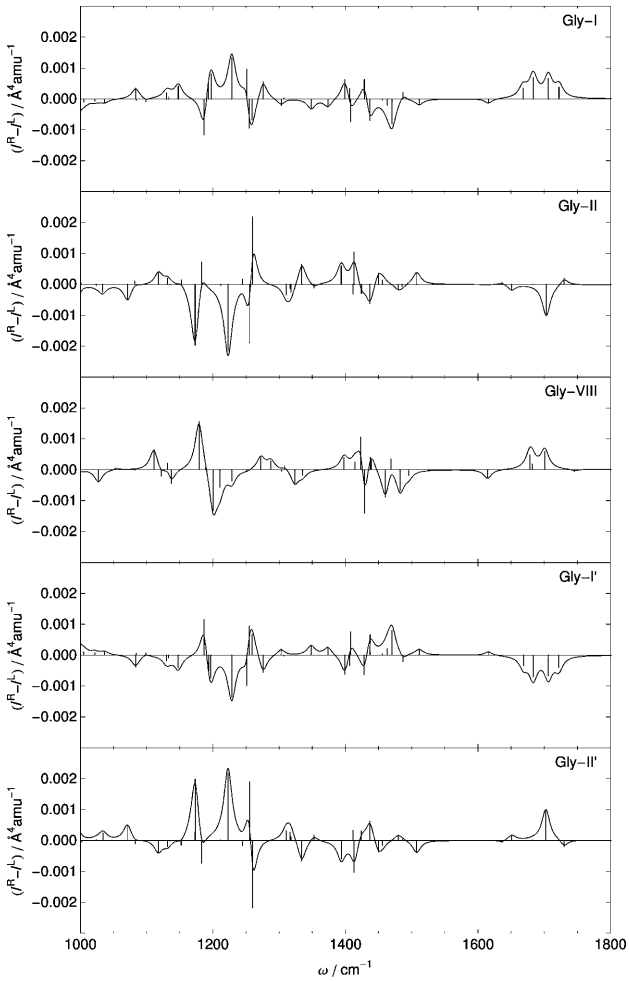

Figure 3. Calculated ROA spectra of the model systems consisting of glycine only (line spectra are scaled by 0.04).

As can be seen by inspection of these spectra, there are no features common to all five glycine β-turns. This can be easily understood because glycine is an achiral amino acid, and, therefore, the chirality of the glycine β-turns stems only from the turn structure itself. However, types I and I′ as well as types II and II′ β-turns are mirror images of each other, that is, they have the same absolute values but opposite signs for their dihedral angles (see Table 3; the slight deviations from exact mirror symmetry are due to the numerical accuracy of the structure optimization). Thus, the resulting ROA spectra of these turns are also mirror images of each other and in any region where we encounter positive intensity for the

type I or II glycine β-turn, we find negative intensity in the case of the type I′ or II′ glycine β-turn, and vice versa.

Therefore, we can already conclude that the signatures proposed in the literature do not occur in all β-turn models investigated herein and, moreover, that it is not possible to find signatures common to *all* possible β-turns. However, for practical applications this is only of minor importance, as several turn types such as I′ or II′ occur only very seldom. On the other hand, turn type I is by far the most important one in the sense that it occurs most often (in the original data set used by Hutchinson and Thornton,[22] about one third of all turns belonged to type I, while in a larger data set used by Koch and Klebe,[23] over 80% of all turns belonged to this class). Thus, identifying spectral features common to type I β-turns would already be very helpful.

4.2. Type I β-Turns

The ROA spectra of all type I β-turns investigated herein are compared to each other in Figure 4. For each of the three signatures proposed in the literature (see Table 1), we find a region where all type I turn spectra have the same sign of the total intensity matching these signatures (these regions are labelled 1, 2, and 3 in Figure 4). First, all three spectra show a negative peak at approximately 1190 cm^{-1}. This is reasonably close to the proposed interval between 1200 and 1220 cm^{-1} for signature 1.

Second, we find a positive intensity roughly between 1220 and 1260 cm^{-1} in all three spectra. For Gly-I and Cys-I there is a positive peak in this region, while for Ala-I there is no normal mode inside this region, but there is a strong positive band at slightly lower wavenumbers. Although the positive intensity region between 1220 and 1260 cm^{-1} common to all three spectra lies outside the interval proposed in the literature for signature 2, ranging from approximately 1260 to 1300 cm^{-1}, we should emphasize that these interval boundaries are to be understood as guiding values rather than sharply defined borders. It is important to state here that it is not possible to unequivocally decide whether a given band in the calculated spectra corresponds to a certain signature proposed in the literature. We can only base our decisions on the wavenumbers and intensities, which, however, has to be done with caution since the simplications made in the calculations (e.g. neglect of solvent effects) can lead to wavenumber shifts of certain bands.

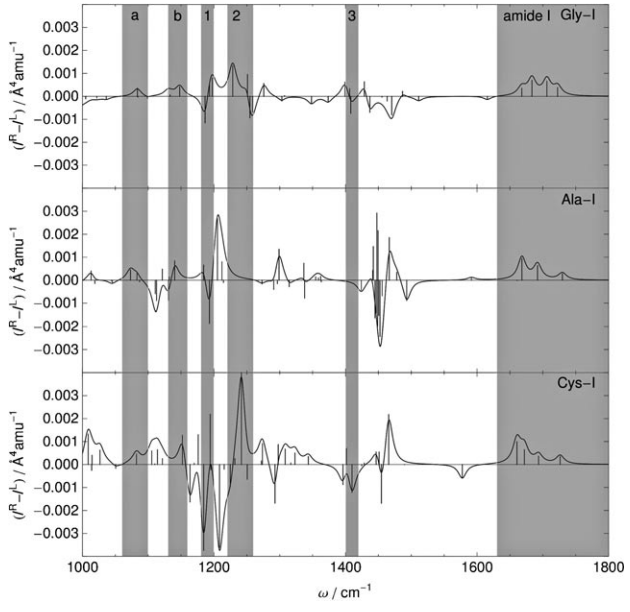

Figure 4. Calculated ROA spectra of the type I β-turn models (line spectra are scaled by 0.04). Wavenumber regions where the total intensity has the same sign in all spectra are highlighted in grey. The signatures labelled 1, 2, and 3 correspond to the three proposed experimental band patterns (Table 1). Additional similarities between all spectra are designated as a and b, respectively.

Finally, negative signals between 1340 and 1380 cm^{-1} (i.e. signature 3) are absent in the spectra of Ala-I and Cys-I, but we find a negative peak at approximately 1400 cm^{-1} common to all three spectra. This is still close to the suggested wavenumber range. Note again that this range has to be understood as a guiding value only. Indeed, in many experimental spectra of polypeptides incorporating β-turns, we observe a negative signal extending above 1380 cm^{-1}.[15,19] Thus, we may conclude that the three signatures for β-turns proposed in the literature can be confirmed in our calculations on type I β-turn models.

Besides these three signatures mentioned in the preceding paragraph one finds additional similarities between the theoretical spectra of the type I β-turn models. There are positive signals both between ~1060 and 1100 cm^{-1} (marked as "a" in Figure 4) and between ~1130 and 1160 cm^{-1} (marked as "b" in Figure 4) in all three spectra. Furthermore, all normal modes in the amide I region between ~1600 and 1800 cm^{-1} are associated with positive ROA intensity in the spectra of the type I β-turns.

We can now investigate whether such peaks are also found in experimental ROA spectra of model β-turns or of proteins containing this secondary structure element. Indeed, we observe positive peaks between ~1060 and 1100 cm^{-1} and between ~1130 and 1160 cm^{-1} in the experimental spectra of α-chymotrypsin, β-lactoglobulin, melanostatin,[17] jack bean concanavalin A, human immunoglobulin G,[7] MS2 capsid,[19] and rabbit metallothionein.[15] However, in most of these spectra, we find a strong couplet, negative at lower wavenumbers and positive at higher wavenumbers, in the amide I region above 1600 cm^{-1} rather than only positive ROA intensity. Nevertheless, it is important to state that in most of these proteins, there are other secondary structure elements present beside β-turns, such as α-helices which are known to yield a couplet in the amide I region.[14] Therefore, all these secondary structure elements contribute to this region.

Thus, our calculations indicate that the signatures shown in Figure 4 might in fact be helpful for a fast yet reliable test for the presence of type I β-turns directly from an ROA spectrum. However, one must keep in mind that such a test can only confirm the *absence* of β-turns from the investigated sample, which is the case when the signatures mentioned above do *not* occur in the spectrum. If they do occur, this does not necessarily indicate the presence of β-turns, as other secondary

structure elements may show similar features. Furthermore, the presence of additional secondary structure elements could lead to a cancellation of β-turn signatures such that one would erroneously conclude their absence. We return to this question in Section 4.6.

4.3. Other β-Turn Types

One can of course investigate the spectra of the other β-turn types in a similar way. For each turn type we can identify several signatures, which are, however, in general not valid for all other turn types. A complete comparison of the spectra for the other types of β-turns can be found in the Supporting Information. In the present context it is worth noting that for all turn types except type II′ one finds a negative total intensity roughly at ~1200 cm^{-1}, that is, for all except the most rare turn type. Note, however, that this negative band is not found exactly at the same position in all spectra. For example, while a negative band is identified between ~1180 and 1200 cm^{-1} for type I turns, a negative signal is found at somewhat higher wavenumbers between ~1210 and 1230 cm^{-1} in the case of type II β-turns. Nevertheless, the normal modes associated with these bands are similar to each other. Thus, we attribute these collectively to signature 1.

Similarly, for all considered types of β-turns we find at least one common negative signal in the region between 1360 cm^{-1} and 1440 cm^{-1}. Even though this negative band appears at different positions in each type of turn, this could be considered as matching signature 3.

However, signature 2 cannot be identified in the other types of β-turns. Only in types I and II′ turns is a matching positive signal between approximately 1260 and 1300 cm^{-1} consistently found for all different side chains. Similarly, the additional signatures a and b identified for type I turns do not show up in most of the other turn types.

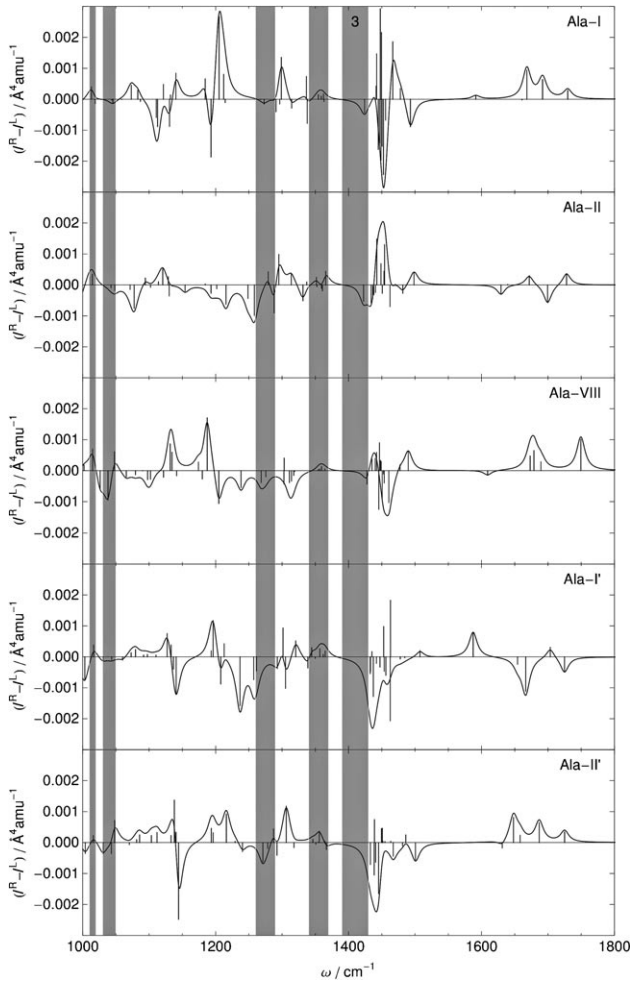

Figure 5. Calculated ROA spectra of the (all-*S*)-alanine β-turn models (line spectra are scaled by 0.04). Wavenumber regions where the total intensity has the same sign in all spectra are highlighted in grey.

4.4. (All-*S*)-Alanine and (All-*S*)-Cysteine Models

Besides investigating signatures for individual turn types, it is interesting to investigate the influence of the amino acid side chains on the ROA spectra. For this, the calculated ROA spectra on sets of β-turn models consisting of (*S*)-alanine and (*S*)-cysteine are shown in Figures 5 and 6, respectively.

First of all, because the configuration of the individual amino acid is the same in all turn models (we choose the naturally occuring (*S*)-form), types I and I′ as well as II and II′, respectively, are no longer enantiomers. Therefore, it is now possible to find spectral features common to all (all-*S*)-alanine β-turns as well as to all (all-*S*)-cysteine β-turns. These are highlighted in Figures 5 and 6, respectively.

For the (all-*S*)-alanine turns, we find a region of negative total intensity common to the spectra of all five turn types between 1390 and 1430 cm^{-1}. This agrees well with the peak identified as signature 3 when comparing the spectra of the type I β-turns. Also for the (all-*S*)-cysteine β-turns, a region with common negative intensity is found at the same position (in this case extending from 1380 to 1430 cm^{-1}). This again confirms that such a negative peak occurs consistently in all the calculated spectra.

In the spectra of (all-*S*)-alanine turns, the peaks identified as signatures 1 and 2 do not show up as a region with the same sign of the total intensity in all five turn types considered. As discussed in the previous section, peaks that might match the signatures proposed in the literature appear for all turn types, but at different positions in each case. In contrast, in the spectra of the (all-*S*)-cysteine β-turns, a common region of negative intensity matching signature 1 is found between 1210 and 1230 cm^{-1}, and a common region of positive intensity matching signature 2 is found between 1300 and 1320 cm^{-1}.

Both for the (all-*S*)-alanine and for the (all-*S*)-cysteine β-turns additional similarities among the different turn types are found. These are marked in Figures 5 and 6. Particularly noteworthy is the region of negative intensity between 1260 and 1290 cm^{-1} in the (all-*S*)-alanine spectra, which might at first sight contradict the above finding that the (positive) signature 2, occurring between 1220 and 1260 cm^{-1}, is valid for all type I β-turns. However, when inspecting the spectrum of Ala-I

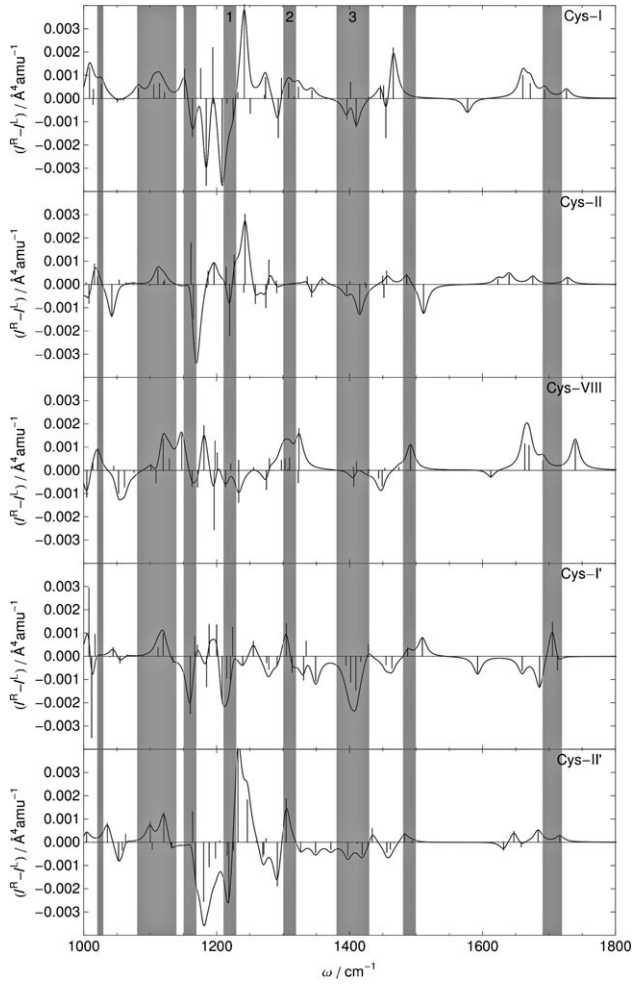

Figure 6. Calculated ROA spectra of the (all-*S*)-cysteine β-turn models (line spectra are scaled by 0.04). Wavenumber regions where the total intensity has the same sign in all spectra are highlighted in grey.

we find a rather strong positive band at 1220 cm^{-1}, which agrees nicely with signature 2, while in fact the wavenumber range between 1260 and 1290 cm^{-1} features a weakly negative total ROA intensity.

When comparing Figures 5 and 6 it is interesting to note that there are more similarities between the spectra of the (all-*S*)-cysteine turn models than for the (all-*S*)-alanine turns. In fact, more and more similarities between the different β-turn types arise when changing the amino acid first from glycine to (*S*)-alanine and then further to (*S*)-cysteine. As a given spectrum is of course always related to the corresponding structure, the five (all-*S*)-cysteine β-turns must be more similar to each other than the five (all-*S*)-alanine β-turns, which in turn are more similar among themselves than the glycine β-turns. Of course, it is not a priori clear whether this increased similarity is associated with the turn-determining secondary structure or whether the common signals are solely due to the side chains.

4.5. Normal Modes Associated with β-Turn Signatures

To verify whether the spectral features we have identified so far are indeed related to the turn structure, we examine the normal modes associated with these signatures. For this, we focus on the normal modes corresponding to the signatures of type I β-turns (see Section 4.2 and Figure 4). In the cases where similar peaks are also found for other types of β-turns, the responsible normal modes are very similar to those found in the type I turns.

Characteristic normal modes together with their corresponding wavenumbers for the most important signatures for type I turns are shown in Figure 7.

The first two signatures, positive ROA intensity between ~1060 and 1100 cm^{-1} (signature a, see Figure 4) and between ~1130 and 1160 cm^{-1} (signature b), respectively, have similar normal modes. Therefore, only characteristic normal modes from signature a are shown in Figure 7a for the Gly-I, Ala-I, and Cys-I model structures. They are highly delocalized over the whole polypeptide backbone of the turn and feature NH in-plane bending for all three β-turns. Additionally, the (all-*S*)-alanine and (all-*S*)-cysteine turns include bending vibrations of the hydrogen atom bonded to the α-carbon atom. This vibration is replaced by a wagging vibration of the methylene (CH_2) group in the case of the glycine β-turn. For this turn, we see a rather strong C^{α}–N stretching vibration which does, however, not occur in the other two β-turns. Finally, we identify deformation vibrations of the methyl side chains in the case of the (all-*S*)-alanine β-turn, while there is a bending vibration of the terminal hydrogen atom bonded to the sulfur atom in the case of the (all-*S*)-cysteine turn.

Signature 1, a negative peak between ~1180 and 1200 cm^{-1}, is caused by the well-known amide III vibrations[27] (which are shown in Figure 7b). These include a strong in-plane bending motion of the hydrogen atom of the amide groups, together with a C–N stretching vibration. For Ala-I and Cys-I, these couple with a C^{α}–H bending vibration, and for Gly-I with a CH_2 twisting vibration.

For signature 2, a positive band between ~1220 and 1260 cm^{-1}, there is no normal mode in the relevant wavenumber range in the case of Ala-I. Here, the positive ROA intensity is rather caused by a strong signal having its maximum approximately at 1205 cm^{-1}. The normal modes underlying this signal represent mostly C^{α}–H bending vibrations coupled to N–H in-plane bending motions.[27] Similar vibrations are found in the normal modes of the glycine and (all-S)-cysteine β-turns. However, for Cys-I the CH_2 groups of the cysteine side chains participate with wagging vibrations in these normal modes.

Then, negative ROA intensity in the region of ~1400 and 1420 cm^{-1} (signature 3) is also a common feature of all three type I β-turns in the case of the glycine and (all-*S*)-cysteine β-turns; the associated normal modes represent CH_2 scissoring vibrations and an umbrella vibration of the methyl unit of the terminal methoxy group (see Figure 7c). As such scissoring vibrations cannot be present in the (all-*S*)-alanine turns (as this amino acid does not incorporate any CH_2 groups), there is only the methyl umbrella vibration contributing to this signature in

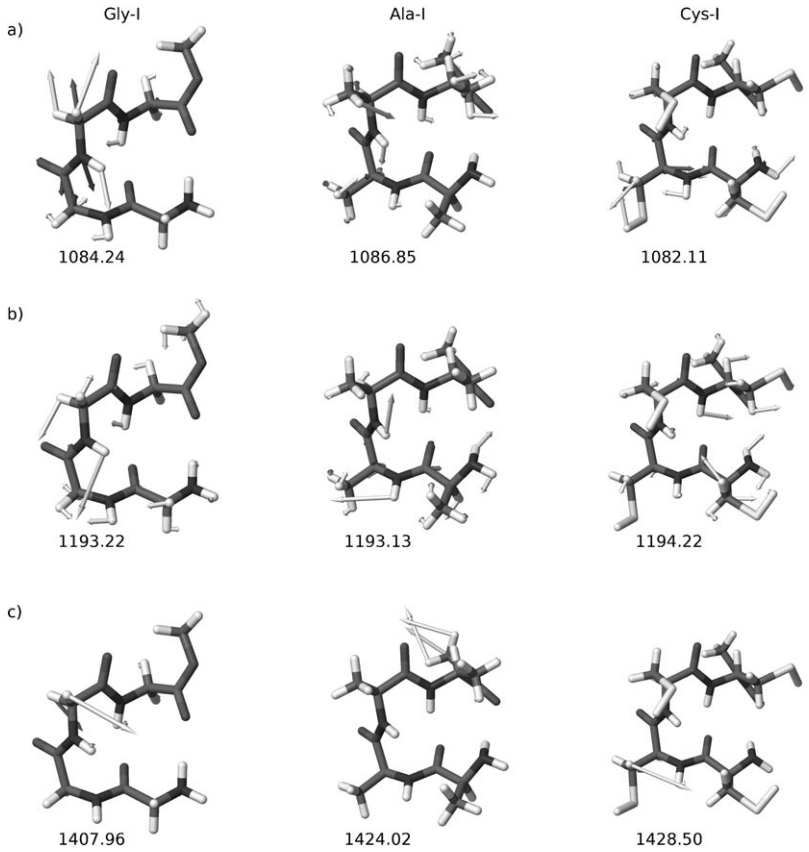

Figure 7. Typical normal modes (and their corresponding wavenumbers) associated with type I β-turn signatures occuring in the wavenumber ranges a) ~1060–1100 cm^{-1}; b) ~1180–1200 cm^{-1}; c) ~1270–1330 cm^{-1}; d) ~1400–1430 cm^{-1}. All wavenumbers are given in cm^{-1}.

the case of the (all-*S*)-alanine β-turn. However, the terminal methoxy group is not an intrinsic feature of a β-turn, but rather has been used here to terminate the polypeptide backbone. We can thus conclude that this feature is caused by the side chains and not by the β-turn structure itself, as the presence of CH_2 groups depends solely on the actual amino acid side chains.

Finally, the positive intensity between ~1630 and 1800 cm^{-1} is also common to all type I β-turn models. This region is associated with the amide I vibrations, that is, a stretching vibration of the carbonyl group (in addition, there is some admixture of C^{α}–H bending). Note also that these normal modes represent rather localized vibrations, in contrast to the other normal modes shown in Figure 7.

4.6. Comparing β-Turns to Other Secondary Structure Elements

Finally it is of crucial importance to compare the signatures identified for β-turns to those of other important secondary structure elements. Only if the proposed signatures do not appear for other secondary structure elements, it will be possible to identify β-turns. An exhaustive comparison of the signatures proposed for the many different secondary structures with the β-turn signatures reported herein is beyond the scope of this work. Therefore, we only compare the ROA spectrum of Ala-I to the calculated spectra of an α- as well as a 3_{10}-helix consisting of 20 (*S*)-alanine residues[14] and check whether or not the turn type I signatures occur in these spectra. The three spectra are shown in Figure 8.

From this comparison, a discrimination between Ala-I and the two helices is possible by means of the type I β-turn signatures. In the α- and 3_{10}-helix spectra, no or only very weak peaks appear between ~1180 and 1230 cm^{-1}. Therefore, the negative peak appearing between ~1180 and 1200 cm^{-1} (signature 1) can be used to clearly distinguish type I β-turns from helices. In contrast to this, positive intensity between approximately 1220 and 1260 cm^{-1}, where signature 2 appears, is also present in the spectrum of the α-helix, where we find positive intensity only above 1250 cm^{-1} as well as in the spectrum of the 3_{10}-helix, where there is a positive peak at about 1250 cm^{-1}. Therefore, sig-

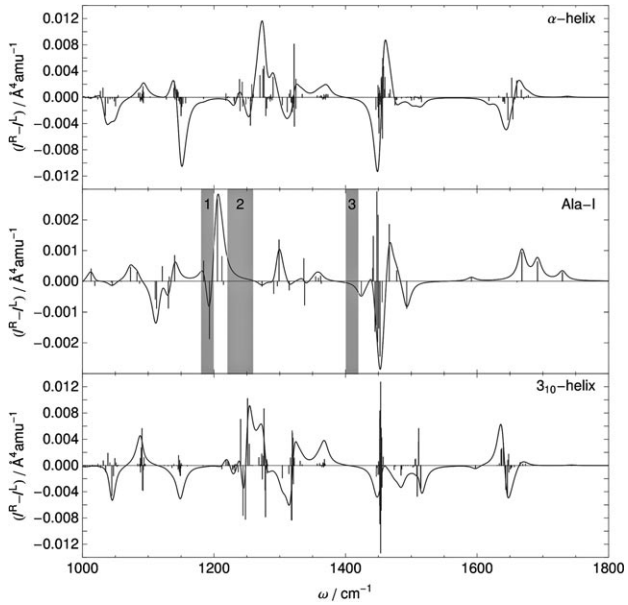

Figure 8. Calculated ROA spectra of an α-helix consisting of 20 (*S*)-alanine residues, Ala-I, and a 3_{10}-helix built from 20 (*S*)-alanine residues (line spectra of the helices are scaled by 0.03, while the line spectrum of Ala-I is scaled by 0.04).

nature 2 is not suited to distinguish the Ala-I β-turn from the two helices.

Another clear signature for distinguishing the Ala-I model structure from the two helices is found in the amide I region between 1600 and 1800 cm^{-1}. Here, we find only positive peaks in the spectrum of Ala-I, while we identify a couplet in the spectra of the two helices. Note that this couplet is negative at lower wavenumbers and positive at higher wavenumbers in the case of the α-helix, while it is positive at lower wavnumbers and negative at higher wavenumbers for the 3_{10}-helix.[14] Thus, by means of this spectral feature we are able to differentiate between α-helices, 3_{10}-helices, and β-turns. However, the presence of multiple secondary structure elements in one protein can be expected to lead to a rather complicated amide I region such that the amide I region might not be very useful in this case.

5. Conclusions and Outlook

In the present work, ROA signatures of β-turns have been investigated by means of quantum chemical calculations on model compounds. First, the signatures proposed in the literature to be characteristic of β-turns have been analyzed in more detail. These are a negative band between ~1200 and 1220 cm^{-1} (signature 1), a positive signal in the range of ~1260 to 1300 cm^{-1} (signature 2), and negative intensity between ~1340 and 1380 cm^{-1} (signature 3).

For type I β-turns (which are the most important type of β-turns since they occur most often), it was found that these signatures are indeed valid for all models studied herein. Furthermore, peaks matching these three signatures can be found in all spectra of the (all-*S*)-cysteine turns. Two of these signatures, namely a negative signal at about 1200 cm^{-1} (signature 1) and a negative signal roughly at ~1400 cm^{-1} (signature 3), occur also in most of the other types of β-turns and thus appear suitable for a test for the presence of β-turns. Signature 1 is associated with amide III vibrations (i.e. an NH in-plane bending vibration coupled with a CN stretching vibration) delocalized over the whole polypeptide backbone of the turn. Signature 3, negative ROA intensity between ~1390 and 1430 cm^{-1}, is found in all spectra of the (all-*S*)-alanine and (all-*S*)-cysteine β-turns. However, these normal modes represent mostly CH_2 scissoring vibrations and an umbrella vibration of the methyl unit of the terminal methoxy group, which is not an intrinsic feature of the β-turn. Thus, it can be expected that these are highly dependent on the actual side chains of the amino acid residues forming the turn.

Moreover, further similarities between the spectra of the same type of β-turn, but with different side chains, have been identified. For example, positive ROA intensity in the amide I region (i.e. the wavenumber range between ~1600 and 1800 cm^{-1}) appear to be a good indication of type I β-turns. In addition, positive peaks between ~1060 and 1100 cm^{-1} and between ~1130 and 1160 cm^{-1} are found for all type I β-turn models considered here.

The analysis employed herein is phenomenological in nature and thus very related to common experimental approaches. Of course, the theoretical methods used in this study permit investigations on isolated, that is, pure, β-turns, the structure of which is exactly known. Nevertheless, the analysis presented here does not allow for a deeper understanding of the origin of the identified signatures. Such insight, however, can be obtained by additional theoretical work. For example, one could analyze the normal modes associated with the β-turn signatures in terms of localized modes.[16,26] On the basis of such an analysis, simplified models describing these characteristic normal modes could be developed.[27] However, for the present case of β-turn structures, such a model is already quite complicated and thus considered for future work.

None of the model systems investigated herein takes solvation effects into account. However, the generic ROA signals arising from such β-turns can, of course, be well analyzed with such an approach and the isolated-molecule approach is a mandatory first step towards a complete understanding of the ROA signals from a molecule in solution. But the inclusion of the solvent in the detailed description of polypeptide ROA spectra remains an important issue and work along this direction is currently in progress in our laboratory.

Computational Details

All structures investigated herein were first fully optimized with the TURBOMOLE 5.10 program package[28] employing density functional theory[29] using the BP86 exchange–correlation functional[30,31] and Ahlrichs' valence triple-zeta basis with two sets of polarization functions (def-TZVPP)[32] on all atoms. In all calculations advantage was taken of the resolution-of-the-identity technique (RI) with the corresponding auxiliary basis sets.[33–35]

Normal modes, harmonic vibrational wavenumbers, and the derivatives of the polarizability tensors required for the ROA backscattering intensities were calculated using the program SNF.[13,36] The analytic energy gradients needed for the seminumerical calculation of the harmonic force field were calculated with TURBOMOLE for distorted structures. The harmonic wavenumbers obtained were *not* scaled since it is known that BP86 yields harmonic wavenumbers which are in good agreement with the corresponding fundamental wavenumbers observed in the experiment,[37,38] which is due to a systematic error cancellation effect.[39]

The polarizability tensors required for the ROA backscattering intensity were obtained using our local[13] version of TURBOMOLE's ESCF module[40–45] employing the same density functional and basis set as described above. To ensure gauge invariance, the velocity representation of the electric dipole operator was applied for the calculation of the $\beta(\mathbf{G}')^2$ invariant. The ROA intensities were obtained using a wavelength of 799 nm. In all cases, it was verified computationally that this wavelength lies well below any electronic excitations (the lowest excitation energy was for all structures in the range of 280–370 nm).

Several studies on the basis-set and density-functional dependence of the ROA wavenumbers and intensities exist,[13,46] which allows for an easy yet reliable calculation of these spectra without the need for cumbersome and time consuming evaluations of many different combinations of basis sets and density functionals. Luber and Reiher showed that a def-TZVPP basis set is necessary in general,[13] especially when the $\beta(\mathbf{G}')^2$ invariant is calculated in the velocity representation as the convergence is much slower in this

case. In this work, we therefore use the def-TZVPP basis set for all ROA calculations. However, for bigger systems than the ones investigated herein the smaller def-TZVP basis set is often preferred for feasibility reasons.[14,15]

The line spectra obtained following this procedure were convoluted with a Lorentzian band featuring a full width at half maximum (FWHM) of 15 cm^{-1} to simulate line broadening due to a not further specified environment. The line broadening as well as the analysis and graphical representation of all vibrational spectra were done with the computer algebra system MATHEMATICA 7.0.[47] Pictures of molecular structures were prepared with CHEMDRAW[48] and JMOL.[49]

Acknowledgements

This work has been supported by the Swiss National Science Foundation SNF (project 200020-132542/1). C.R.J. thanks the DFG-Center for Functional Nanostructures.

Keywords: chirality · computational chemistry · density functional calculations · proteins · Raman spectroscopy

[1] G. Bringmann, T. Bruhn, K. Maksimenka, Y. Hemberger, *Eur. J. Org. Chem.* **2009**, 2717 – 2727.
[2] L. Whitmore, B. A. Wallace, *Nucleic Acids Res.* **2004**, *32*, W668 – W673.
[3] L. D. Barron, A. D. Buckingham, *Mol. Phys.* **1971**, *20*, 1111 – 1119.
[4] P. W. Atkins, L. D. Barron, *Mol. Phys.* **1969**, *16*, 453 – 466.
[5] L. D. Barron, M. P. Bogaard, A. D. Buckingham, *J. Am. Chem. Soc.* **1973**, *95*, 603 – 605.
[6] W. Hug, S. Kint, G. F. Bailey, J. R. Scherer, *J. Am. Chem. Soc.* **1975**, *97*, 5589 – 5590.
[7] L. D. Barron, L. Hecht, E. W. Blanch, A. F. Bell, *Prog. Biophys. Mol. Biol.* **2000**, *73*, 1 – 49.
[8] R. R. Ernst, G. Bodenhausen, A. Wokaun, *Principles of Nuclear Magnetic Resonance in One and Two Dimensions*, Clarendon Press, Oxford, **1987**.
[9] F. Zhu, N. W. Isaacs, L. Hecht, L. D. Barron, *Structure* **2005**, *13*, 1409 – 1419.
[10] M. N. Kinalwa, E. W. Blanch, A. J. Doig, *Anal. Chem.* **2010**, *82*, 6347 – 6349.
[11] T. Helgaker, K. Ruud, K. L. Bak, P. Jørgensen, J. Olsen, *Faraday Discuss.* **1994**, *99*, 165 – 180.
[12] M. Pecul, K. Ruud, *Int. J. Quantum Chem.* **2005**, *104*, 816 – 829.
[13] S. Luber, M. Reiher, *Chem. Phys.* **2008**, *346*, 212 – 223.
[14] C. R. Jacob, S. Luber, M. Reiher, *Chem. Eur. J.* **2009**, *15*, 13491 – 13508.
[15] S. Luber, M. Reiher, *J. Phys. Chem. B* **2010**, *114*, 1057 – 1063.
[16] C. R. Jacob, M. Reiher, *J. Chem. Phys.* **2009**, *130*, 084106.
[17] Z. Q. Wen, L. Hecht, L. D. Barron, *Protein Sci.* **1994**, *3*, 435 – 439.
[18] F. Zhu, N. W. Isaacs, L. Hecht, G. E. Tranter, L. D. Barron, *Chirality* **2006**, *18*, 103 – 115.
[19] I. H. McColl, E. W. Blanch, A. C. Gill, A. G. O. Rhie, M. A. Ritchie, L. Hecht, K. Nielsen, L. D. Barron, *J. Am. Chem. Soc.* **2003**, *125*, 10019 – 10026.
[20] E. Smyth, C. D. Syme, E. W. Blanch, L. Hecht, M. Vašák, L. D. Barron, *Biopolymers* **2001**, *58*, 138 – 151.
[21] K.-C. Chou, *Anal. Biochem.* **2000**, *286*, 1 – 16.
[22] E. G. Hutchinson, J. M. Thornton, *Protein Sci.* **1994**, *3*, 2207 – 2216.
[23] O. Koch, G. Klebe, *Proteins* **2009**, *74*, 353 – 367.
[24] V. M. Naik, S. Krimm, *Int. J. Peptide Protein Res.* **1984**, *23*, 1 – 24.
[25] C. Herrmann, K. Ruud, M. Reiher, *ChemPhysChem* **2006**, *7*, 2189 – 2196.
[26] C. R. Jacob, S. Luber, M. Reiher, *J. Phys. Chem. B* **2009**, *113*, 6558 – 6573.
[27] T. Weymuth, C. R. Jacob, M. Reiher, *J. Phys. Chem. B* **2010**, *114*, 10649 – 10660.
[28] R. Ahlrichs, M. Bär, M. Häser, H. Horn, C. Kölmel, *Chem. Phys. Lett.* **1989**, *162*, 165 – 169.
[29] O. Treutler, R. Ahlrichs, *J. Chem. Phys.* **1995**, *102*, 346 – 354.
[30] A. D. Becke, *Phys. Rev. A* **1988**, *38*, 3098 – 3100.
[31] J. P. Perdew, *Phys. Rev. B* **1986**, *33*, 8822 – 8824.
[32] F. Weigend, M. Häser, H. Patzelt, R. Ahlrichs, *Chem. Phys. Lett.* **1998**, *294*, 143 – 152.
[33] K. Eichkorn, F. Weigend, O. Treutler, R. Ahlrichs, *Theor. Chem. Acc.* **1997**, *97*, 119 – 124.
[34] K. Eichkorn, O. Treutler, H. Öhm, M. Häser, R. Ahlrichs, *Chem. Phys. Lett.* **1995**, *240*, 283 – 290.
[35] K. Eichkorn, O. Treutler, H. Öhm, M. Häser, R. Ahlrichs, *Chem. Phys. Lett.* **1995**, *242*, 652 – 660.
[36] J. Neugebauer, M. Reiher, C. Kind, B. A. Hess, *J. Comput. Chem.* **2002**, *23*, 895 – 910.
[37] M. Reiher, J. Neugebauer, B. A. Hess, *Z. Phys. Chem.* **2003**, *217*, 91 – 103.
[38] M. Reiher, G. Brehm, S. Schneider, *J. Phys. Chem. A* **2004**, *108*, 734 – 742.
[39] J. Neugebauer, B. A. Hess, *J. Chem. Phys.* **2003**, *118*, 7215 – 7225.
[40] R. Bauernschmitt, R. Ahlrichs, *Chem. Phys. Lett.* **1996**, *256*, 454 – 464.
[41] R. Bauernschmitt, M. Häser, O. Treutler, R. Ahlrichs, *Chem. Phys. Lett.* **1997**, *264*, 573 – 578.
[42] S. Grimme, F. Furche, R. Ahlrichs, *Chem. Phys. Lett.* **2002**, *361*, 321 – 328.
[43] R. Bauernschmitt, R. Ahlrichs, *J. Chem. Phys.* **1996**, *104*, 9047 – 9052.
[44] H. Weiss, R. Ahlrichs, M. Häser, *J. Chem. Phys.* **1993**, *99*, 1262 – 1270.
[45] F. Furche, D. Rappoport in *Theoretical and Computational Chemistry, Vol. 16* (Ed.: M. Olivucci), Elsevier, Amsterdam, **2005**, chap. III, pp. 93–128.
[46] M. Reiher, V. Liégeois, K. Ruud, *J. Phys. Chem. A* **2005**, *109*, 7567 – 7574.
[47] MATHEMATICA 7.0, Wolfram Research, Inc., Champaign, Illinois, **2008**.
[48] CHEMDRAW ULTRA 11.0, CambridgeSoft, Cambridge, Massachusetts, **2008**.
[49] JMOL, An Open-Source Java Viewer for Chemical Structures in 3D, http://www.jmol.org/.

Received: December 21, 2010
Published online on March 22, 2011

